International Research Journal of Engineering and Technology (IRJET) e-ISSN: 2395 -0056
Volume: 03 Issue: 05 | May-2016 www.irjet.net p-ISSN: 2395-0072

Design and Analysis of Soft-Switching Boost Converter

Mohit Paprikar, Akash Gupta
Department of Electrical Engineering , Maharana pratap College of Technology, Gwalior

Rajive Gandhi proudyogiki vishwavidyalaya ,Bhopal , India

Abstract- ***In this paper a Zero-Current Transition Fourth Order boost converter is proposed which offers significant advantages over conventional second order boost converter. The fourth order converter provides slightly higher voltage gain and the ripple in input current and output voltage is also reduced. The zero current transition cell which is also incorporated into the circuit provides further advantages in terms of reduction of switching losses for nearly all the switching devices. Mathematical analysis of the proposed converter is done to find the various modes of operation and their timings. In order to verify the soft switching performance of this converter simulation is carried out in PSIM. To further test the advantage provided by the proposed converter over hard switched converters a comparative loss analysis is carried out in MATLAB for various load conditions. The converter performance is predetermined for a 12 to 24 V, 30 W prototype in simulation and then compared with experimental results. Experimental measurements are in close agreement with simulations.***

I. Introduction

Dc-dc boost converters are most commonly used to deliver higher load voltages from given low voltage source. The conventional boost converter though suffers from the following disadvantages: (i) Its full load efficiency is low on account of higher switching losses, (ii) High duty ratio even for moderate voltage gain realization (iii) Extreme duty ratio operation unable to yield expected voltage gainIn order to eliminate some of these limitations, higher order boost pulse width modulated (PWM) converter are developed. These converters give higher voltage gain but at higher switching frequencies the full-load efficiency is still a limitation. Recently, more soft-switching techniques are coming-up to overcome the excessive switching losses occurring in the conventional hard-switched dc-dc converters and to realize higher efficiencies for the dc-dc converter at full-load conditions.

To improve the efficiency there are two soft switching schemes were reported in the literature [1]:

1. *Zero voltage switching (ZVS) during turn-ON.*
2. *Zero current switching (ZCS) during turn-off.*

The selection of these schemes is device specific, i.e., MOSFET or IGBT. Although these soft-switching techniques yield better efficiency but, still there are some drawbacks.

The ZCS turn-OFF has drawbacks such as:

- *Significant voltage stress on the main diode.*
- *Increase in the conduction losses.*
- *The resonant inductor in series with the main switch, which increases the magnetic losses.*

To alleviate some of these drawbacks the zero-current transition/ zero-voltage transition (ZCT/ ZVT) techniques have been proposed in literature [1] - [2].

However, there is not enough literature covering the development of soft-switching schemes for fourth-order converters. Therefore, the aim is to improve the efficiency of the fourth order boost converter, belonging to higher order family, through soft-switching using the ZCT technique. Here the soft-switching is realized by integrating the ZCT cell into the fourth-order boost converter. This paper presents some investigations on steady-state analysis and design of one higher-order boost converter, Fourth-order Zero Current Transition Boost Converter (FZCTBC). In a single switching cycle the circuit will undergo seven different modes of operation. The time intervals and the status of each switching device is shown in the table given below.

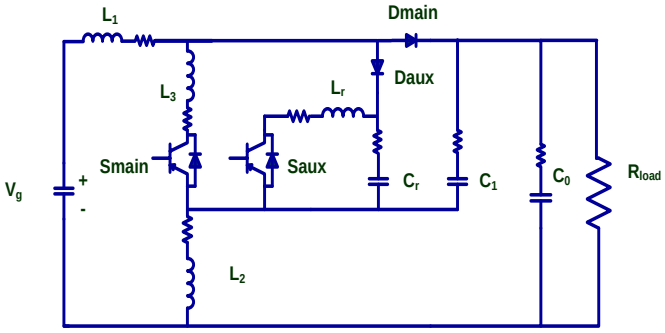

Fig. 1. Circuit diagram of the zero-current transition fourth-order boost converter.

II. Steady-state Analysis of zero-current transition fourth-order boost converter

A. Topological variations in each mode of operation

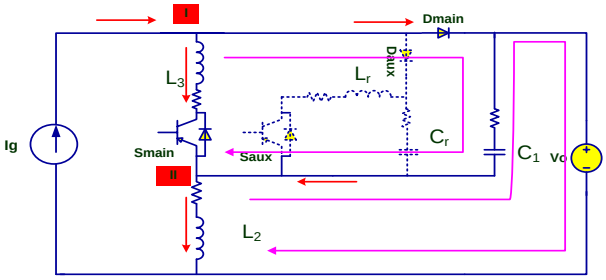

(A) Equivalent circuit during mode-I operation

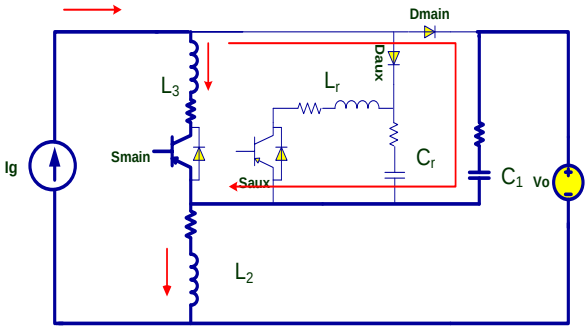

(B) Equivalent circuit during mode-II operation

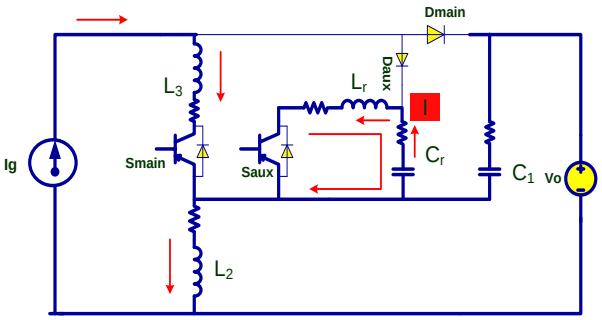

(C) Equivalent circuit during mode-III operation

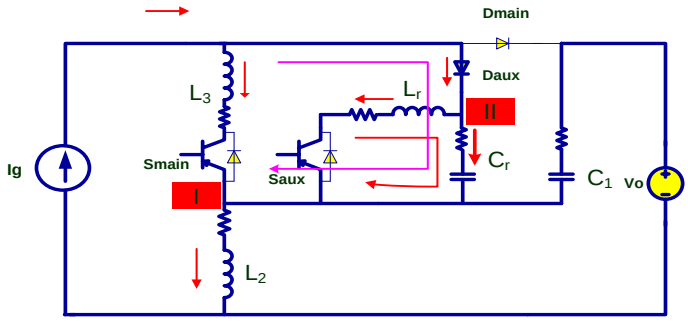

(D) Equivalent circuit during mode-IV operation

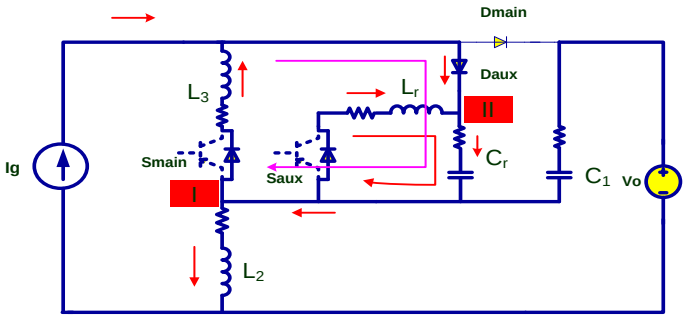

(E) Equivalent circuit during mode-V operation

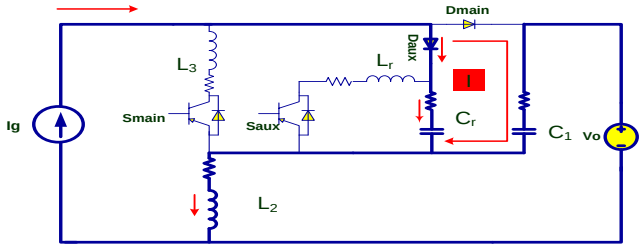

(F) Equivalent circuit during mode-VI operation

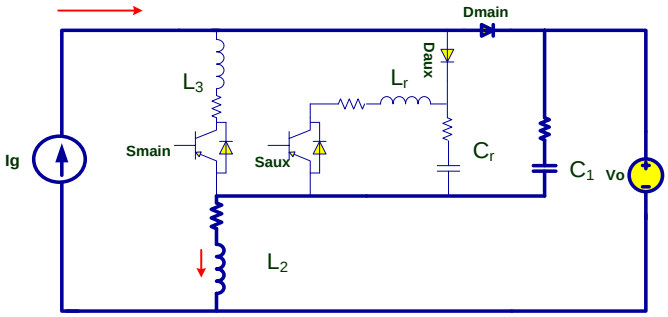

(G) Equivalent circuit during mode-VII operation

Figures 2(A) to 2(g) are operating modes

B. Operation modes:

Mode 1: (to<t<t1)

Initial Conditions:

$V_{cr}(t_0) = V_0'$; $i_{lr}(t_0) = 0$

On writing KCL at node -I

$$I_g = i_{L3} + i_D$$

$$i_{L3}(t) = \frac{V_0}{(L_2 + L_3)} t \quad \text{.....(1)}$$

Main diode current, $i_D = I_g - i_{L3}$

$$i_D(t) = Ig - \frac{V_0}{(L_2 + L_3)} t \quad \text{.....(2)}$$

And at ,t=t1,
iL3(t)=Ig,On equating,

$$t_1 = \frac{I_g (L_2 + L_3)}{V_0} \quad \text{.....(3)}$$

Mode 2: (t1<t<t2)

In this mode a steady state current equal to Ig flows through the main switch, and this mode continues till the auxiliary switch is fired ,
During this mode the main diode stage will be,

$$v_{L_3} + v_{C_1} - v_{D\,main} = 0$$

(as iL3 reached steady state value Ig)

$$\mathbf{v_{D_{main}}(t) = v_{C_1} t}$$

Mode 3: (t2<t<t3)
Initial conditions:

$$V_{cr}(t_1) = V_o'; \qquad i_{lr}(t_1) = I_g + I_o$$

Applying KCL:

$$i_{L_r} = i_{c_r}$$

$$L_r \frac{d^2 i_{lr}}{dt^2} = \frac{dV_{cr}}{dt}$$

On solving the above two equations,

$$vc_r(t - t_2) = V_0 \cos w_r (t - t_2) \quad \text{....(4)}$$

$$iL_r(t) = -\frac{V_0}{Z_r} \sin \omega_r t \quad \text{.....(5)}$$

Where

$$\omega_r = \frac{1}{\sqrt{L_r C_r}}; \qquad Z_r = \sqrt{\frac{L_r}{C_r}}$$

At $t = t_3$ *, at the end of this mode* $vc_r(t_3) = 0$

$$\cos \omega r(\Delta t_3) = \cos \frac{\pi}{2}$$

$$t_3 - t_2 = \frac{\pi}{2} \sqrt{L_r c_r} \quad \text{.....(6)}$$

On KVL,

$$-vL_3 + vc_r - v_{D_{aux}} = 0$$

As vc_r *getting discharged and hence* $v_{D_{aux}} = 0$ *When*
$vc_r(t) = 0, vL_3 = 0, \because iL_3 = I_g$, *steadyvalue*

And hence auxiliary diode starts conducting by the end of this mode, and with this circuit enters into the next mode of operation

Mode 4: (t3<t<t4):

$$iL_3(0) = I_g$$

$$iL_3 + i_{d\,aux} = iL_2$$

$$i_{dau\,x} = iL_2 - iL_3$$

$$\frac{diL_2}{dt} = -\frac{vc_r}{L_r}$$

On KVL,

$$vc_r = vL_3$$

On KCL,

$$i_{L3} = I_g - i_{daux}$$

On solving above equations,

$$v_{cr}(t) = \frac{-V_0 S\,in(\omega_r (t_3 - t_2))}{\sqrt{1 + \frac{L_r}{L_3}}} S\,in(\omega_0 (t - t_3)) \quad \text{.....(7)}$$

Where $\omega_o = \sqrt{\frac{L_3 + L_r}{c_r L_r L_3}}$

And main switch current, is given by

$$i_{L3}(t) = I_g - \frac{V_0}{\omega_o L_3 \sqrt{1 + \frac{L_r}{L_3}}} \frac{\sin \omega_r (t_3 - t_2)}{(1 - Cos\omega_o (t - t_3)} \quad \text{.....(8)}$$

But, at $t = t4$
At the end of this mode,

$$i_{L3}(t) = 0$$

$$I_g = \frac{V_0}{L_3} \frac{\sin \omega_r (t_3 - t_2)}{\omega_o L_3 \sqrt{1 + \frac{L_r}{L_3}}} (1 - Cos\omega_o (t - t_3)$$

$$t_4 = t_3 + (\frac{1}{\omega_o})Cos^{-1}((\frac{-I_g\omega_o L_3\sqrt{1+L_r/L_3}}{V_o Sin\omega_r(t_3-t_2)})+1) \quad .....(9)$$

Mode 5: (t4<t<t5)

During this mode,

$$v_{Lr} = -v_{cr}$$

$$= \frac{V_o}{z_r} - \frac{V_0 \sin\omega_r(t_3-t_2)}{L_r\omega_0\sqrt{1+\frac{L_r}{L_3}}}(\cos(\omega_o(t-t_4))-1)$$

At the end of this mode at $t = t_5$,

$i_{Lr}(t_5) = 0$,

On solving,

$$t_5 = t_3 + (\frac{1}{\omega_o})(\pi + Cos^{-1}(-1+(\frac{\omega_o\sqrt{1+L_r/L_3}}{\omega_r Sin\omega_r(t_3-t_2)}))) \quad .....(10)$$

Mode 6: (t5<t<t6)

During this mode the main diode voltage will be falling as the resonating capacitor is charging.
On KCL at node-I,
ic=Ig

$$C_r\frac{dvc}{dt} = I_g$$

$$vc(t^1) = \frac{I_g}{C_r}(t-t_5) + \frac{V_o\sin\omega_r(t_3-t_2)}{\sqrt{1+\frac{L_r}{L_3}}}\sin\omega_o(t-t_3) + \frac{I_g}{C_r}(t-t_5) \quad .....(11)$$

On KVL along-I,
Vdmain=Vo+vcr

$$v_{dmain}(t^1) = V_O + \frac{V_o\sin\omega_r(t_3-t_2)}{\sqrt{1+\frac{L_r}{L_3}}}\sin\omega_o(t-t_3) + \frac{I_g}{C_r}(t-t_5) \quad .....(12)$$

At the end of this mode, at t=t6, when vcr charges upto Vo,main diode comes into conduction,i.e $v_{dmain}(t_6) = 0$,

$$0 = V_O + \frac{V_o\sin\omega_r(t_3-t_2)}{\sqrt{1+\frac{L_r}{L_3}}}\sin\omega_o(t_6-t_3) + \frac{I_g}{C_r}(t-t_5)$$

$$t_6 = t_5 + (C_r(V_o - V_o\frac{(Sin\omega_r(t_3-t_2))(Sin\omega_o(t_5-t_4)}{I_g(\sqrt{1+L_r/L_3})} \quad ..(13)$$

Mode 7: (t6<t<TS)

During this mode main diode curent reaches a steady state value and this mode continues till the main switch is turned ON.

At, $t_7 = T_s$ *.....(14)*

This mode is identical to the freewheeling stage of the conventional boost converter

The time minimum and maximum Ontimes for SA gate signal has to satisfy the following to satisfy ZCT condition.

$$Dsaux\min = \pi\frac{\sqrt{L_rC_r}}{2} + \pi\sqrt{L_{eq}C_r}$$

$$Dsaux\max = \pi\frac{\sqrt{L_rC_r}}{2} + 2\pi\sqrt{L_{eq}C_r}$$

Where , $L_{eq} = \frac{L_3 * L_r}{L_3 + L_r}$

III. Design of ZCT-Fourth-Order Boost Converter

A. Power stage components design:

The converter is designed with the following specifications: Load nominal rated power Po=30W,Load Voltage Vo=24 V,Switching frequency,fs=100 KHz., Load Voltage Ripple<5%,Input Current ripple=<10%. Final Power Stage elements Designed are: The parameters of the designed converter to meet the specifications (ΔIL1 <10% ΔVo<5%) are: L1=150 µH, L2=50 µH, C1=100 µF, C2=100 µF,.

B. Resonant Tank Circuit Design:

Here, a simple design procedure is followed as explained below. From ZCS boost normalized switching frequency(fns) Vs. Gain(M) characteristics, for a voltage gain of 2.0 it is observed the combinations of normalized switching frequency and Q(Normalized load) and chosen to be for a Q=12,the fns=0.2.By using the design equation as mentioned from (14) to (16) Lr and Cr have been obtained
As Lr=0.6µH,and Cr=170 n F.

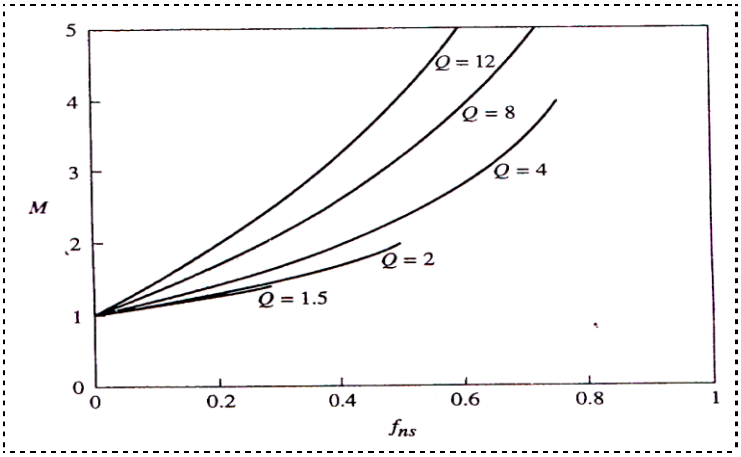

*Fig. 3.(a).*ZCS Boost converter Gain Vs. Normalized switching frequency Characteristics.

$$Z_o = \frac{R_o}{Q} \quad \text{.....(14)}$$

Resonant frequency, $fr = \frac{f_s}{f_{ns}}$

$$\text{Resonat Inductor, } L_r = \frac{Z_o}{\omega_r} \quad \text{.....(15)}$$

$$\text{Re}\,sonatCapacitor, C_r = \frac{1}{Z_O \omega_r} \quad \text{.....(16)}$$

And minimum and maximum Duty for the auxiliary switch can be obtained as 0.13 to 0.2.

The combination and range of resonant tank circuit have been investigated and the range is as below.

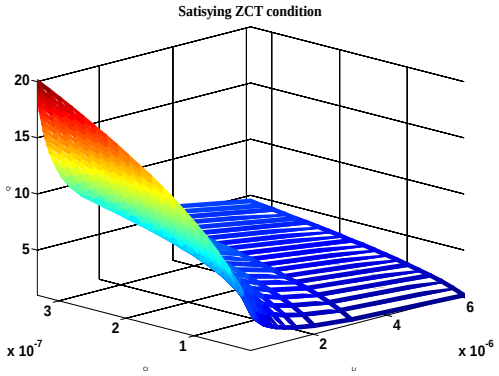

Fig.3.b.Resonant tank circuit elements for satisfying ZCT condition

IV. Simulation And Experimental Results

A 30 Watt prototype FZCTBC system has been designed to verify the effectiveness of the soft-switching/ZCT performance of the proposed converter and its controller regulation capability. The converter is supplied from a battery of 12 V and the desired load voltage is 24 V. The parameters of the designed converter to meet the specifications (ΔIL1 <10% ΔVo<5%) are: L1=150 µH, L2=50 µH, Lr=0.6 µH, Cr=170 nF, C1=100 µF, C2=100 µF, R= 19.2 Ω, fs = 100 kHz. Zero-current transition/ soft-switching performance of the proposed boost converter is verified through PSIM simulations [10] and for illustration purpose steady-state current and voltage waveforms of main/ auxiliary switch/ diode SM/ SA and DM/ DA are shown in Figs. 3.(a) to 3.(d). It is clear from these waveforms that the main and auxiliary switches are turning-OFF only after their drain to source Current is dropping to zero, i.e ZCT turn-OFF. Furthermore, the main diode and auxiliary diode are turning-ON at zero voltage switching (ZVS). In order to verify the simulation results a 12 -to- 24 V, 30 W laboratory prototype, converter parameters listed above, has been designed. The devices used in the prototype converter circuit are: Switch IRFP250N, Diode MUR1520, Driver circuit IR2110 and Opto-isolator-6N137.

For nominal/ extreme conditions of duty ratio the converter ZCT performance has been verified. To demonstrate this ZCT feature, a 12 V supply is connected to source and then various currents / voltage waveforms have been recorded. Soft-switching ON-OFF transition under zero current turn-OFF of the switching devices (SA and SM) while zero-current turn-OFF of the diodes (DA and DM) as shown in Figs. 4b and 5b.

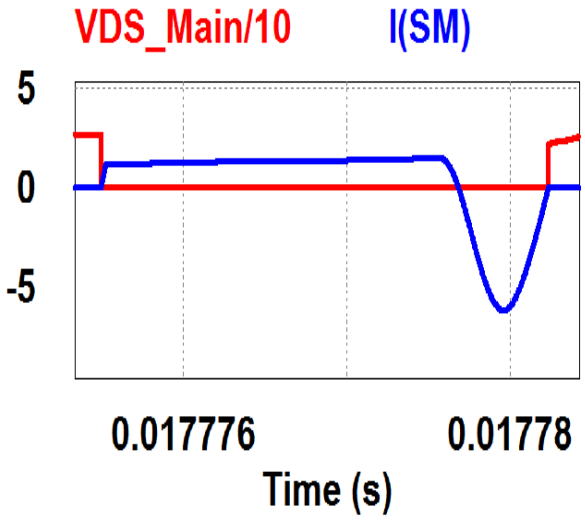

Fig. 4.(a) Zero-Current turn OFF of the main switch.

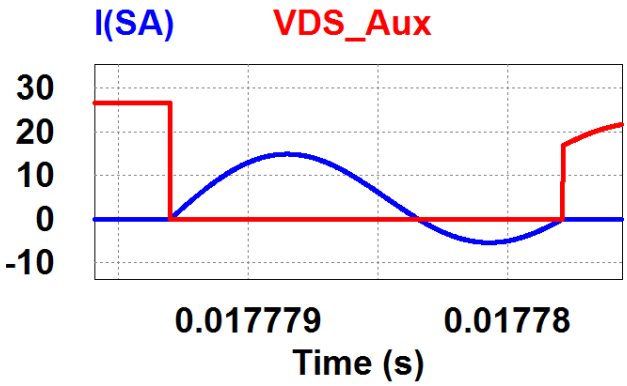

Fig. 4.(b) Zero-Current turn OFF of the main switch.

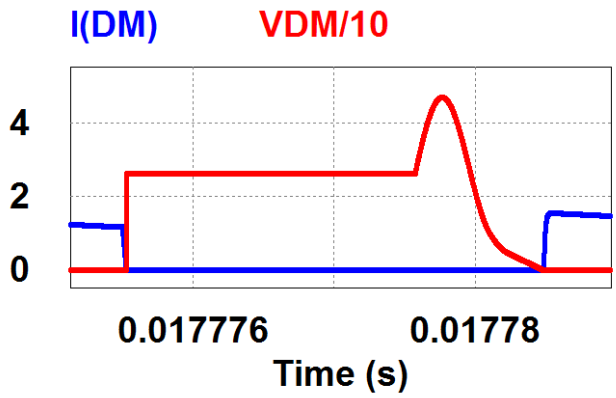

Fig. 4.(c) Zero Voltage turn-ON of the main diode.

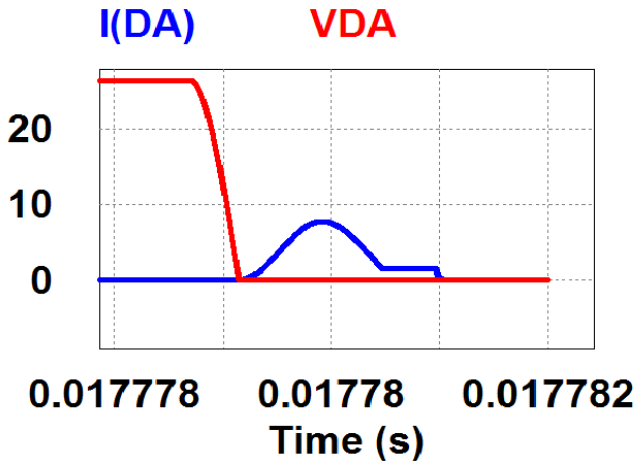

Fig. 4.(d) Zero Voltage turn-ON and Zero Current turn –OFF of the main diode.

V. Conclusion

In this paper a soft-switching fourth order boost converter operating modes have been established and then zero-current turn-OFF of main switch/Aux. switch and zero-current turn-OFF of diodes were verified. FZCTBC has been designed for and its validity is verified both in simulation and experiment. Theoretical analysis results were in close agreement with the experimental measurements.

References

[1] *Guichao Hua, Eric X. Yang, Yimin Jiang, and Fred C. Lee, "Novel Zero-current-transition PWM Converters", 0-7803-1243-0/93$03.00 Q 1993 IEEE.*

[2] *Mummadi Veerachary," Digital Controller Design for Fourth-Order Boost Converter", 978-1-4673-2605-6/12/ © 2012 IEEE.*

[3] *K. H. Liu and F. C. Lee, "Zero-voltage switching technique in DC/DC converters," IEEE Trans. Power Electron., vol. 53, pp. 293– 304, July1990.*

[4] *G. Hua, C. S. Leu,Y. Jiang, and F. C. Lee, "Novel zero-voltage-transition PWM converters," IEEE Trans. Power Electron., vol. 9, pp. 213–219,Mar. 1994.*

[5] *Hang-Seok Choi,Bo Hyung Cho," Novel zero-current-switching (ZCS) PWM switch cell minimizing additional conduction loss", IEEE transactions on Industrial Electronics, vol. 49, no. 1, February 2005*

[6] *K. Wang, F. C. Lee, G. Hua, and D. Borojevic, "A comparative study of switching losses of IGBT's under hard-switching, zero-voltage-switching and zero-current switching," in Proc. IEEE PESC'94, 1994, pp. 1196–1204.*

[7] *K. Wang, G. Hua, and F. C. Lee, "Analysis, design and ZCS-PWM boost converters," in Proc. IEEJ Int. Power Electronics Conf., 1995, pp.1202–1207.*

[8] *Power Electronic Circuits. By---Issa Batarseh.*

[9] *MATLAB, user manual, 2005.*

[10] *PSIM, user manual, 2005.*

[11] *dSPIC30F2020, Microchip, user manual, 2009.*